ISBN: 978-3-95450-261-5 ISSN: 2673-7000 doi: 10.18429/JACoW-NAPAC2025-TUP037

ENHANCING RECIPROCAL SPACE RESOLUTION IN MEV ULTRAFAST ELECTRON DIFFRACTION WITH PERMANENT MAGNET LENSES

C. J. R. Duncan*, T. Xu, R. J. England
SLAC National Accelerator Laboratory, Menlo Park, CA, USA
B. Guzelturk, Argonne National Laboratory, Lemont, IL, USA
P. Denham, P. Musumeci, University of California, Los Angeles, Los Angeles, CA, USA

Abstract

Ultrafast electron diffraction (UED) probes structural dynamics on femtosecond timescales and angstrom spatial scales. Artificial crystals are a novel experimental target for UED beams. Typically composed of lattice-mismatched atomic layers, the repeating atomic patterns in artificial crystals can have periods several nanometers in length, which produces intricate satellite features in the electron diffraction pattern. Resolving fascinating satellite diffraction peaks in a compact UED beamline requires high angular magnification. In this work, we describe the implementation of post-sample angular magnification using a pair of compact permanent magnet solenoid lenses. Configured as an objective-eyepiece pair, these lenses achieve a camera length of 50 meters, i.e., the lens system is equivalent to extending the beamline drift length by a factor 15. We demonstrate the advantages of this scheme with data that resolves satellite diffraction peaks in a heterostructure sample.

INTRODUCTION

The dominant features in electron diffraction from single-crystal samples are typically the Bragg peaks corresponding to the few-Angstrom size of the crystal unit cell. More subtle features of particular scientific interest are caused by periodic distortions in the crystal lattice (PLD). These distortions can be intrinsic to a material, e.g., charge-density waves [1], and also engineered via interfacial strain in stacked heterostructures, the latter being especially significant in samples consisting of only a few atomic layers [2].

The period of PLD can extend to several nanometers [2], and thus measuring the diffraction peaks corresponding to PLD requires especially fine reciprocal space resolution [3]. While the ultimate physical limit on reciprocal space resolution is set by the brightness of the electron beam source, the detector point-spread-function and pixel size are an important practical contraint that can be overcome by magnifying the diffraction pattern on the detector. Angular magnification can be characterized by the *camera length* L, defined,

$$L = \frac{dr}{d\theta}, \tag{1}$$

where θ is the scattering angle (or other deflection) at the sample plane and r is the transverse position of the scattered (deflected) beam on the detector plane. When imaging system is simply a drift section of the beamline, L is the drift length.

* cjduncan@slac.stanford.edu

An angular magnification lens doublet implemented at the SLAC Megaelectronvolt UED facility is shown in Fig. 1. A permanent magnet solenoid (PMS) objective lens with a focal length of 62 cm at the 3.1 MeV primary energy of the beam forms a virtual image of the sample diffraction pattern that is further magnified by a 3 cm focal length eyepiece. The short focal length PMS is further described in Table 1, and described in more detail in [4, 5].

Table 1: Permanent Magnet Solenoid Parameters

Remanence	1.32 T
Inner radius	0.6 cm
Outer radius	3.5 cm
Length of single ring	1.6 cm
Focal length (single ring, 3.1 MeV)	5.0 cm
Focal length (double ring, 3.1 MeV)	2.7 cm

RESULTS

To demonstrate the improvement in reciprocal space resolutuion, Fig. 2 shows an example static diffraction pattern from a strontium titanate / lead zirconate (STO/PZO) heterostructure without (a) and with (b) the angular-magnification lens system. Knowing the STO lattice constant and beam energy determines $d\theta$ in Eq. (1), from which the camera length is calculated to be 50 m, a factor 15 longer than the physical distance from source to detector.

Lineouts shown in Fig. 2(c) and (d) are fit to the function $I(x)$:

$$\begin{aligned} &I(x; A_1, \mu_1, \sigma_1, \gamma_1, A_2, \mu_2, \sigma_2, \gamma_2) \\ &= A_1 V(x - \mu_1; \sigma_1, \gamma_1) + A_2 V(x - \mu_2; \sigma_2, \gamma_2), \end{aligned} \tag{2}$$

where $V(x; \sigma, \gamma)$ is the Voigt profile, a convolution of a normalized gaussian with r.m.s. size σ and a normalized lorentzian with f.w.h.m. of γ [6]. The fits demonstrate that with angular magnification (panel (d)), the measured width of the diffraction peak is reduced by a factor two compared to without (panel (c)). The residual peak width in the magnified case is explained by the coherence length of the illuminating beam and the crystallinity of the sample.

Figure 3(a) zooms in on the diffraction feature at Miller index (0,-2), plotting contours of equal diffraction intensity. These contours reveal the presence of satellite features associated with the interfacial strain between the STO and PZO, which have mismatched lattice constants. The satellites are

ISBN: 978-3-95450-261-5 ISSN: 2673-7000 doi: 10.18429/JACoW-NAPAC2025-TUP037

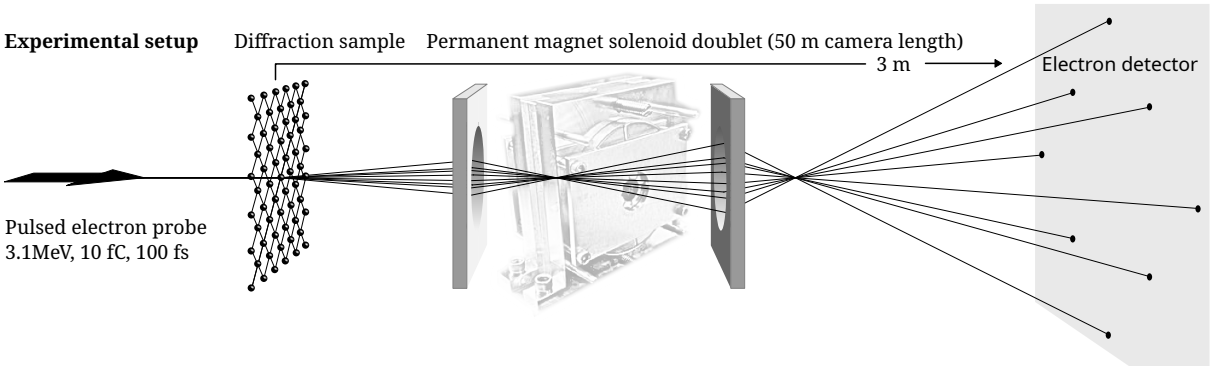

Figure 1: Angular magnification setup: from left to right, the femtosecond diffraction probe is incident on a STO/PZO heterostructure. Scattered rays are collected by an objective lens and a diffraction pattern forms at the back focal plane of the objective. An second, eye piece lens forms a magnified image of the diffraction pattern. The lens doublet is characterized by it's 50 m camera length, defined in the main text.

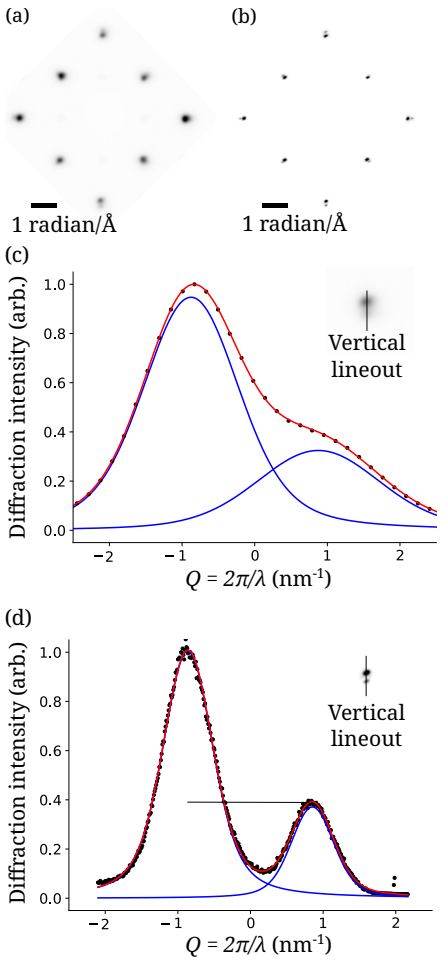

Figure 2: Diffraction pattern of the STO/PZO heterostructure sample without (a) and with (b) the lens doublet shown in Fig 1. (c) Without the lens doublet, lineout of the diffraction feature at the Miller index (0,-2) fit to a sum of Voigt profiles. (d) The same lineout with the lens doublet inserted shows a factor 2 improvement in reciprocal space resolution.

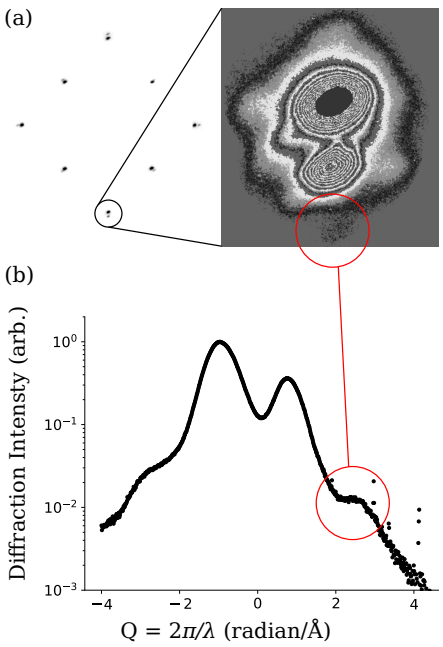

Figure 3: (a) Diffraction intensity contours of the feature at Miller index (0,-2), indicating the presence of diffraction satellite peaks. (b) Logarithmic plot of the lineout reveals the intenisty of these satellite features.

partly obscured by the tails of the main Bragg peaks; a distinct satellite is highlighted in red. Figure 3(b) shows the same lineout as Fig. 2(b) but on a logarithmic scale, indicating that the satellites are at least a factor 100 weaker in intensity than the main Bragg peaks.

CONCLUSION

The results reported here show the practical advantages of a permanent magnet lensing system for angular magnification in UED experiments. The Bragg contributions of the seperate STO and PZO layers of the sample are clearly distinct, and tails in the scattering distribution reveal the

ISBN: 978-3-95450-261-5 ISSN: 2673-7000 doi: 10.18429/JACoW-NAPAC2025-TUP037

presence of satellite peaks associated with periodic strain. The satellite peaks could be resolved with enhanced contrast in future work by more aggressively collimating the probe beam.

ACKNOWLEDGEMENTS

This work was supported by the U.S. Department of Energy Office of Science, Office of Basic Energy Sciences under Contract No. DE-AC02-76SF00515. The SLAC MeV-UED program is supported by the U.S. Depratment of Energy Office of Science, Office of Basic Energy Sciences under FWP 10075, FWP 100713, FWP 100940, and FWP 101293.

REFERENCES

[1] S. Vogelgesang *et al*., "Phase ordering of charge density waves traced by ultrafast low-energy electron diffraction", *Nat. Phys.* vol. 14, no. 2, p. 184, Nov. 2018. doi:10.1038/nphys4309

[2] S. H. Sung, *et al*., "Torsional periodic lattice distortions and diffraction of twisted 2D materials", *Nat. Commun.* vol. 13, no. 1, p. 7826, Dec. 2022. doi:10.1038/s41467-022-35477-x

[3] C. J. R. Duncan, *et al.,* "Multi-scale time-resolved electron diffraction: A case study in moiré materials", *Ultramicroscopy* vol. 253, p. 113771, Nov. 2023. doi:10.1016/j.ultramic.2023.113771

[4] T. Xu, *et al.,* "Focusing of Relativistic Electron Beams with Permanent Magnetic", 2025, arXiv:2504.21121 [physics.acc-ph]. doi:10.48550/arXiv.2504.21121

[5] P. Denham, "High Energy Electron Diffraction Instrument with Tunable Camera Length", *Struct. Dyn.* vol 11. p. 024302, Mar. 2025. doi:10.1063/4.0000240

[6] L. P. René de Cotret, B. J. Siwick, "A general method for baseline-removal in ultrafast electron powder diffraction data using the dual-tree complex wavelet transform", *Struct. Dyn.* vol. 4 no. 4. p. 044004, Mar. 2017. doi:10.1063/1.4972518